

## SWTY—A general peptide probe for homogeneous solution binding assay of 14-3-3 proteins

Meng Wu<sup>a</sup>, Brian Coblitz<sup>a</sup>, Sojin Shikano<sup>a</sup>, Shunyou Long<sup>a</sup>, Lisa M. Cockrell<sup>b</sup>,  
Haian Fu<sup>b</sup>, Min Li<sup>a,\*</sup>

<sup>a</sup> Department of Neuroscience and High Throughput Biology Center, School of Medicine, Johns Hopkins University, 733 North Broadway, Baltimore, MD 21205, USA

<sup>b</sup> Department of Pharmacology, Emory University School of Medicine, Atlanta, GA 30322, USA

Received 28 August 2005

Available online 15 December 2005

### Abstract

Dimeric 14-3-3 proteins exert diverse functions in eukaryotes by binding to specific phosphorylated sites on diverse target proteins. Critical to the physiological function of 14-3-3 proteins is the wide range of binding affinity to different ligands. The existing information of binding affinity is mainly derived from nonhomogeneous-based methods such as surface plasmon resonance and quantitative affinity precipitation. We have developed a fluorescence anisotropy peptide probe using a genetically isolated 14-3-3-binding SWTY motif. The synthetic 5-(and-6)-carboxyfluorescein(FAM)-RGRSWpTY-COOH peptide, when bound to 14-3-3 proteins, exhibits a seven-fold increase in fluorescence anisotropy. Different from the existing assays for 14-3-3 binding, this homogeneous assay tests the interaction directly in solution. Hence it permits more accurate determination of the dissociation constants of 14-3-3 binding molecules. Protocols for a simple mix-and-read format have been developed to evaluate 14-3-3 protein interactions using either purified recombinant 14-3-3 fusion proteins or native 14-3-3s in crude cell lysate. Optimal assay conditions for high-throughput screening for modulators of 14-3-3 binding have been determined.

© 2005 Elsevier Inc. All rights reserved.

**Keywords:** 14-3-3; Fluorescence anisotropy; Binding assay; High-throughput screening; Dissociation constant; SWTY

Ubiquitous in all eukaryotic cells, dimeric 14-3-3 proteins have numerous binding partners and are involved in diverse physiological functions including signal transduction, apoptosis, protein trafficking and localization, metabolism, cell motility, and malignant transformation (see reviews [1–3]). At the biochemical level, isoforms of 14-3-3 proteins appear to be quite similar in binding specificity. Increasing evidence suggests the potential of isoform-specific functions [4,5]. Furthermore, 14-3-3 proteins have been used as diagnostic markers for prion-related diseases such as Creutzfeldt–Jakob disease or mad cow disease [6]. Because of the critical role in signaling pathways, 14-3-3

proteins also represent potential targets for therapeutic intervention in cancer [7].

Essential to most 14-3-3 functions is the ability to recognize a short peptide substrate only upon phosphorylation. As the first protein module with preferential affinity to phosphorylated substrates, 14-3-3 binding provides an inducible mechanism of translating signal-activated phosphorylation into protein–protein interaction. With respect to substrate consensus, RSx(pS/pT)xP and RxΦx(pS/pT)xP (Φ as an aromatic or aliphatic amino acid, x as any amino acid) are two canonical consensus binding motifs for 14-3-3, also referred to as mode I and mode II binding motifs [8,9]. Recent evidence shows that 14-3-3 protein also recognizes certain C-terminal sequences [10–12]. However, the reported affinity values of these C-terminus-mediated interactions were considerably weaker than

\* Corresponding author. Fax: +1 410 614 1001.

E-mail address: [minli@jhmi.edu](mailto:minli@jhmi.edu) (M. Li).

typical mode I or mode II interactions [10,12]. Using a genetic selection of a random peptide library, a potent C-terminal forward trafficking signal, RGRSWTY-COOH, has been identified and is recognized by 14-3-3 proteins with much higher affinity than those previously reported [13,14]. This mode of binding has a consensus of (pT/pS)<sub>x</sub><sub>1-2</sub>-COOH and is now termed mode III [11], and the peptide similarly recognizes the same binding pocket [13]. In addition, nonphosphorylated 14-3-3 binding motifs have been reported (for example, [15,16]). Thus, determination of binding affinity is important to address the functional role in the physiological context.

While ranking order of relative affinity for different interactions is valuable information, the critical and diverse roles of 14-3-3 proteins often require accurate assessment of the absolute affinity. However, except for a few peptides that have been measured with solution-based methods such as isothermal titration microcalorimetry (ITM)<sup>1</sup> assay [12], most reported dissociation constants ( $K_D$ ) were obtained by quantitative affinity precipitation or label-free technologies such as surface plasmon resonance (SPR). While these assays are adequate in assessing the relative affinity, solid-phase binding assays often lead to overestimating binding affinity as seen in interactions between peptides and PDZ domains [17]. A recent report of 14-3-3-mediated interaction with histone revealed a difference of as much as 1000-fold between  $IC_{50}$  obtained from SPR and  $K_D$  from ITM [18]. As a result, the values obtained by different methods also are difficult to compare. Furthermore, most of these methodologies are usually not compatible with a high-throughput screening (HTS) format.

We have identified a novel 14-3-3 binding peptide, RGRSWpTY-COOH (termed SWTY), and employed it for affinity determination [13,14]. Here we present the development and characterization of a homogeneous fluorescence anisotropy binding assay for 14-3-3 using a fluorescein-conjugated SWTY peptide. The assay is compatible with both purified 14-3-3 proteins and native 14-3-3 proteins in crude cell lysate. The broad adaptability and robust signal for a variety of targets supports general applicability.

<sup>1</sup> Abbreviations used: AANAT, arylalkylamine *N*-acetyltransferase; BMH, yeast 14-3-3; AHA2, *Arabidopsis* plasma membrane H<sup>+</sup>-ATPase; Chaps, 3-[(3-cholamidopropyl)dimethylammonio]-1-propanesulfonate; DMSO, dimethyl sulfoxide; ExoS, ADP-ribosyltransferase exoenzyme S; FI, fluorescence intensity; FRET, Förster resonance energy transfer or fluorescence resonance energy transfer; GF14 $\omega$ , plant 14-3-3 (tobacco); Hepes, 4-(2-hydroxyethyl) piperazine-1-ethanesulfonic acid; ITM, isothermal titration microcalorimetry; LOD, limit of detection; PMA2, plasma membrane H<sup>+</sup>-ATPase; RBA, radioactive binding assay; SPR, surface plasmon resonance; SWTY, RGRSWTY or its phosphorylated sequences; PBS, phosphate-buffered saline; BSA, bovine serum albumin; HTS, high-throughput screening.

## Materials and methods

### Reagents and chemicals

All inorganic salts were of analytical purity and were obtained from Sigma–Aldrich (St. Louis, MO) unless otherwise stated. All solutions were prepared in a 10 mM 4-(2-hydroxyethyl)piperazine-1-ethanesulfonic acid (Hepes) buffer (pH 7.3) unless otherwise described.

### Preparation and purification of recombinant 14-3-3 proteins

Human 14-3-3 $\zeta$  protein was expressed as a hexahistidine-tagged fusion from a T7-driven promoter and purified from *Escherichia coli* strain BL21-SI (Invitrogen, Carlsbad, CA) according to procedures provided by the manufacturer.

### Synthesis of fluorescein-labeled peptide probes and unlabeled peptides

The synthesized peptides are summarized in Table 1. 5- (and 6)-Carboxyfluorescein-labeled peptide FAM-RGRSWpTY-COOH and control sequences RGRSWpTY-COOH, RGRSWTY-COOH, RGRSWpTE-COOH, RGRSWpTD-COOH, RGRSWpTP-COOH, RGRSWpTG-COOH, RGRSWpTYP-COOH, RGRSWpTYA-COOH, LSQRQRSTpSTPNVHA-COOH, INRSApSEP-COOH, Biotin-(AHA)<sub>2</sub>-TIQSYpTV-COOH, and Biotin-(AHA)<sub>2</sub>-TIQRSYpTV-COOH were synthesized (New England Peptides, Boston, MA or Abgent, San Diego, CA). The R18 peptide, with a sequence of PHCVPRDLSWLDLEA NMCLP, was purchased from Biomol International (Plymouth Meeting, PA). The peptides were prepared as stock solutions by dissolving in water and if necessary with the addition of a minimal amount of acetonitrile. The working

Table 1  
 $K_D$  of the peptides with 14-3-3 $\zeta$

Peptide sequences	Abbreviation	$K_D \pm SD$ ( $\mu$ M)
FAM-RGRSWpTY-COOH	FAM-SWpTY	0.49 $\pm$ 0.14
H <sub>2</sub> N-RGRSWpTY-COOH	SWpTY	0.17 $\pm$ 0.04
H <sub>2</sub> N-RGRSWTY-COOH	SWTY	>100
H <sub>2</sub> N-RGRSWpTE-COOH	SWpTE	3.4 $\pm$ 0.2
H <sub>2</sub> N-RGRSWpTP-COOH	SWpTP	45 $\pm$ 11
H <sub>2</sub> N-RGRSWpTG-COOH	SWpTG	1.5 $\pm$ 0.01
H <sub>2</sub> N-RGRSWpTD-COOH	SWpTD	2.2 $\pm$ 0.3
H <sub>2</sub> N-RGRSWpTYP-COOH	SWpTYP	0.16 $\pm$ 0.07
H <sub>2</sub> N-RGRSWpTYA-COOH	SWpTYA	0.34 $\pm$ 0.10
H <sub>2</sub> N-LSQRQRSTpSTPNVHA-COOH	pS-Raf259	12.8 $\pm$ 4.8
H <sub>2</sub> N-INRSApSEP-COOH	pS-Raf621	>100
Biotin-(AHA) <sub>2</sub> -TIQSYpTV-COOH	QSYpTV	6.0 $\pm$ 2.0
Biotin-(AHA) <sub>2</sub> -TIQRSYpTV-COOH	RSYpTV	2.5 $\pm$ 1.0
H <sub>2</sub> N-PHCVPRDLSWLDLEANMCLP-COOH	R18	0.39 $\pm$ 0.30

solutions for the affinity detection were prepared in the 10 mM Hepes buffer (pH 7.3).

### Fluorescence detection

For both the fluorescence-intensity-based and the fluorescence-anisotropy-based affinity detections, a multifunctional plate reader Safire<sup>2</sup> (Tecan US, Research Triangle Park, NC) was used. The detection was performed on 384-well black-walled microplates in fluorescence polarization measurement mode. The excitation was set at 470 nm and the emission at 525 nm, with 20-nm bandwidth for emission. The time between move and flash was set at 100 ms with three reads per well. G factor was determined as 1.1 by calibration of 100 nM FAM-RGRSWpTY-COOH as 20 mP for fluorescence polarization, with buffer solution as the reference.

### Determination of the equilibrium dissociation constant ( $K_D$ ) of the fluorescein-labeled peptide

For fluorescence-anisotropy-based affinity detections with FAM-RGRSWpTY-COOH, the dissociation constant ( $K_D$ ) of FAM-RGRSWpTY-COOH with 14-3-3 $\zeta$  was determined by the titration of 100 nM of FAM-RGRSWpTY-COOH in a 100- $\mu$ l total volume 30 min after the addition of different concentrations of 14-3-3 $\zeta$ , with one binding site fitting with Eq. (1) using Origin 7.0 (Northampton, MA). In the fitting,  $y = r - r_0$ , with  $r$  as fluorescence anisotropy of FAM-RGRSWpTY-COOH with the addition of 14-3-3 $\zeta$ ,  $r_0$  as FAM-RGRSWpTY-COOH alone, and  $x$  as the concentration of 14-3-3 $\zeta$

$$y = \frac{B * x}{K_{D_{FAM-SWPpTY}} + x} \quad (1)$$

### Competitive binding assays for unlabeled peptides

Competitive experiments were employed for the  $K_D$  measurements of unlabeled control peptides using procedures similar to an earlier report [17]. Briefly, competitive anisotropy experiments were performed with premixed test sequences and 800 nM FAM-RGRSWpTY-COOH. Upon addition of 0.65  $\mu$ M of 14-3-3 $\zeta$  in a total volume of 100  $\mu$ l, the anisotropy was determined after 120 min unless otherwise indicated. The fitting was done using Origin 7.0 with Eq. (2) with  $y = (r - r_0)/(r_{max} - r_0)$  as bound fraction,  $r$  as fluorescence anisotropy of FAM-RGRSWpTY-COOH with the addition of 14-3-3 $\zeta$ ,  $r_0$  as FAM-RGRSWpTY-COOH alone,  $r_{max}$  as the maximum of fluorescence anisotropy of FAM-RGRSWpTY-COOH with the addition of 14-3-3 $\zeta$ ,  $D_0$  as the concentration of FAM-RGRSWpTY-COOH,  $P_0$  as the concentration of 14-3-3 $\zeta$ ,  $K_{D_{FAM-SWPpTY}}$  (0.49  $\mu$ M) as  $K_D$  for FAM-SWPpTY as detected earlier in this paper,  $K_{D_{control}}$  as  $K_D$  for control sequences, and  $x$  as the concentrations of control peptides

$$y = \frac{1}{2 * D_0} * \left\{ \left( \frac{K_{D_{FAM-SWPpTY}}}{K_{D_{control}}} * x + K_{D_{FAM-SWPpTY}} + D_0 + P_0 \right) - \sqrt{\left( \frac{K_{D_{FAM-SWPpTY}}}{K_{D_{control}}} * x + K_{D_{FAM-SWPpTY}} + D_0 + P_0 \right)^2 - 4 * D_0 * P_0} \right\} \quad (2)$$

### Cell lysate preparation

Cell lysate was prepared as previously described [19]. HEK 293 cells confluent in a 10-cm dish were washed with PBS, scraped, and transferred to a 25-ml tube. After centrifugation at 1000g for 5 min at room temperature, the cells ( $2.2 \times 10^6$ ) were resuspended in 10 ml Hepes buffer and ultrasonicated 10 times for 10-s durations with 30-s intervals on ice (Branson Sonifier 450; Branson, Danbury, CT). After centrifugation at 10,000g for 10 min at 4 °C, the supernatant was stored in aliquots at -20 °C. The protein concentrations in the cell lysate were determined by the Bradford assay [20] in 96-microwell plates with BSA as a calibration standard (Bio-Rad, Hercules, CA).

### 14-3-3 detection in cell lysate

The native 14-3-3 proteins in cell lysate were measured by fluorescence anisotropy 30 min after the addition of 400 nM FAM-RGRSWpTY-COOH into 45  $\mu$ l of crude cell lysate to a total volume of 100  $\mu$ l in 384-well black-walled microplates. The calibration curve was generated by spiking known amounts of recombinant 14-3-3 $\zeta$  into the denatured lysates in a total volume of 100  $\mu$ l. The denatured lysate was obtained by incubating the crude cell lysate at 100 °C for 10 min. The denatured lysate was used to assess the nonspecific effect on anisotropy in the absence of specific 14-3-3 binding to the labeled peptide probe.

The native 14-3-3 proteins in cell lysate were alternatively determined by immunoblotting. The cell lysate was run on a 12% polyacrylamide gel, transferred to a nitrocellulose membrane, and blotted with anti-14-3-3 Ab (Zymed, South San Francisco, CA) followed by HRP-conjugated secondary Abs (Vectorlab, Burlingame, CA). The immunoblotting signal was developed with the ECL system (Amersham-Pharmacia, Piscataway, NJ). The immunoblotted bands were detected by a Fuji Luminescent Image Analyzer (LAS 3000, Fujifilm, Valhalla, NY) and quantitated by the Multi Gauge program (Fujifilm). The amount was determined by plotting with the signals obtained with known amounts of recombinant 14-3-3 proteins.

### High-throughput screening evaluation

For the evaluation of the binding assay for its compatibility with high-throughput screening, a robotic liquid handling system (Biomek 2000; Beckman Coulter, Fullerton, CA) has been applied for the addition of solutions into the 384-well black microplates.

The Z factor was calculated using Eq. (3) [21] with SD as standard deviation and  $A_v$  as the average of FAM-RGRSWpTY-COOH alone and FAM-RGRSWpTY-COOH saturated with 14-3-3 $\zeta$ . Each set comprises 20 data points

$$Z = 1 - \frac{|SD_1 + SD_2| * 3}{|Av_1 - Av_2|} \quad (3)$$

## Results

### Spectra characterization of the probes

N-terminally labeled fluorescein peptide, FAM-RGRSWpTY-COOH, has spectra typical of fluorescein (Fig. 1A). In contrast to other reports using environment-sensitive fluorophores, addition of 14-3-3 $\zeta$  led to a decrease of fluorescence intensity rather than an increase (Figs. 1A and C). This may be due to pH sensitivity of FAM-RGRSWpTY (see Fig. 4). The spectra display no obvious change, consistent with the notion that the fluores-

cein has no strong interaction with the 14-3-3. In the presence of 14-3-3 $\zeta$ , an approximately seven-fold increase of the anisotropy was detected (Fig. 1B), providing a desirable signal-to-noise ratio. The signal of anisotropy was both 14-3-3 and FAM-RGRSWpTY-COOH peptide dependent. No signal was detected by a binding mutant of 14-3-3 $\zeta$  (K49E) (Fig. 1B) [13].

To evaluate the stability of the anisotropy signal, time course measurements were performed. Fig. 2 shows that the anisotropy signal reached a plateau within 10 min for FAM-RGRSWpTY-COOH and it remained constant up to 120 min or longer. All measurements reported here were done within 30 min unless otherwise described to avoid prolonged irradiation that could potentially introduce photobleaching to the fluorescent probe.

### Assay sensitivity to solvent conditions

The experimental conditions for the binding assay have been characterized in several aspects including ionic strength and  $Mg^{2+}$ , detergent, and protein concentration.

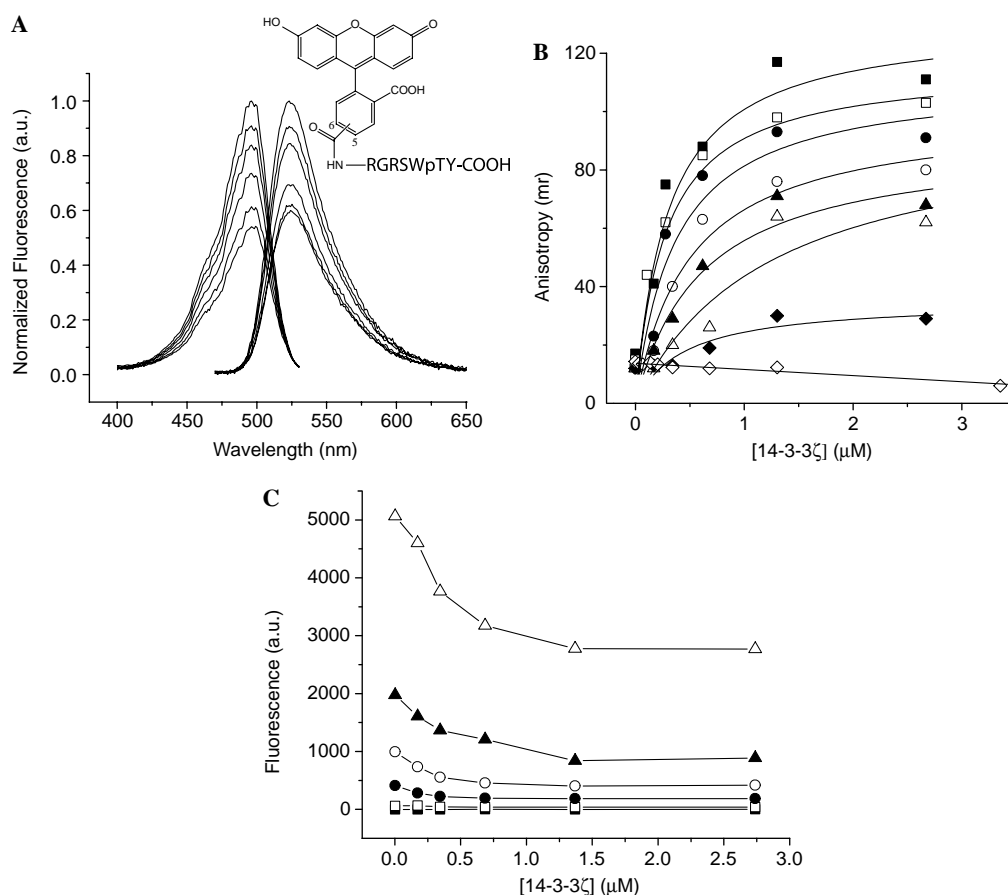


Fig. 1. Fluorescent spectra of fluorescein-labeled peptide (FAM-RGRSWpTY-COOH). (A) Normalized excitation (left) and emission (right) spectra of FAM-RGRSWpTY-COOH (5.0  $\mu$ M) with increasing concentrations of 14-3-3 $\zeta$  from 0, 0.17, 0.34, 0.68, 1.37, and 2.74  $\mu$ M (top to bottom) in a total volume of 100  $\mu$ l. The inset shows the structure of FAM-RGRSWpTY-COOH. (B) Anisotropy titration of increasing concentrations of FAM-RGRSWpTY-COOH from 0.05 (■), 0.1 (□), 0.2 (●), 0.3 (○), 1.0 (▲), 2.0 (△), and 5.0 (◆)  $\mu$ M (top to bottom) with 14-3-3 $\zeta$  in a total volume of 100  $\mu$ l. The line indicated with unfilled diamonds (◇) is the anisotropy titration of 0.08  $\mu$ M FAM-RGRSWpTY-COOH with 14-3-3 $\zeta$  K49E binding mutant. (C) Fluorescence intensity titration of 14-3-3 $\zeta$  with increasing concentrations of FAM-RGRSWpTY-COOH from 0 (■), 0.1 (□), 0.3 (●), 1 (○), 2 (▲), and 5 (△)  $\mu$ M (bottom to top) in a total volume of 100  $\mu$ l.

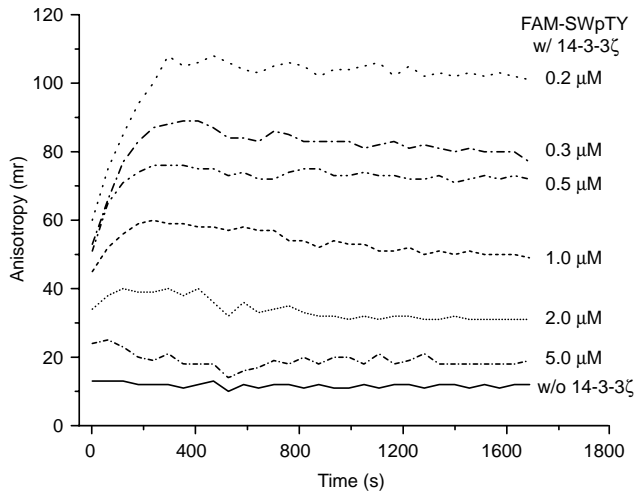


Fig. 2. Kinetic response of the anisotropy titration of FAM-RGRSWpTY-COOH with 14-3-3 $\zeta$ . Time course of anisotropy signal of increasing concentrations of FAM-RGRSWpTY-COOH from 0.2, 0.3, 0.5, 1.0, 2.0, and 5.0  $\mu$ M. The concentration of 14-3-3 $\zeta$  is kept at 2.74  $\mu$ M in a total volume of 100  $\mu$ l. The bottom line is the time course of the anisotropy of 0.8  $\mu$ M FAM-RGRSWpTY-COOH in the absence 14-3-3 $\zeta$ .

The potential effect by ionic strength was tested with different concentrations of sodium chloride. The concentration of NaCl has minimal effect on the anisotropy (Fig. 3A).

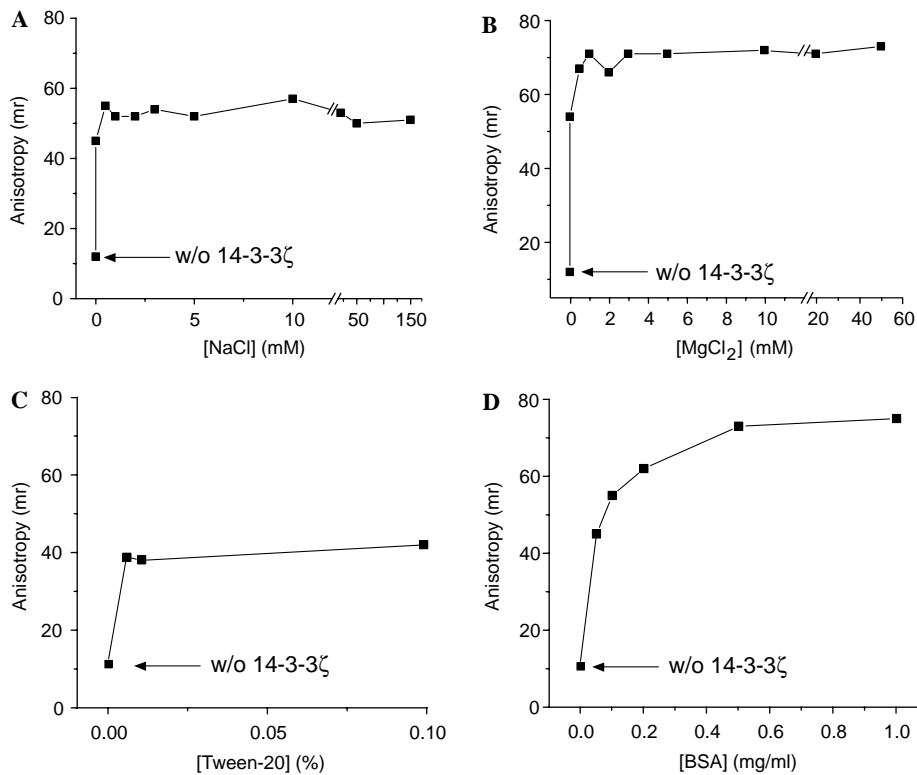


Fig. 3. Assay sensitivity to experimental conditions. (A) Anisotropy signal (vertical axis) is plotted against increasing concentrations of NaCl (horizontal axis). (B) Anisotropy signal (vertical axis) is plotted against increasing concentrations of MgCl<sub>2</sub> (horizontal axis). (C) Anisotropy signal (vertical axis) is plotted against increasing concentrations of Tween 20 (horizontal axis). (D) Anisotropy signal (vertical axis) is plotted against increasing concentrations of bovine serum albumin (BSA) (horizontal axis). The experiments were performed with 0.8  $\mu$ M FAM-RGRSWpTY-COOH and 0.68  $\mu$ M 14-3-3 $\zeta$  in a total volume of 100  $\mu$ l. All experiments were repeated at least three times.

Divalent metal ions, such as Mg<sup>2+</sup>, were reported for certain effects on the binding [22]. In the concentration range tested, Mg<sup>2+</sup> could only marginally increase the anisotropy, but the effect was quite consistent in the concentration range between 2 and 50 mM (Fig. 3B). In contrast, the detergent Tween 20 resulted in a decreased anisotropy signal by  $\sim$ 30% (Fig. 3C). Application of 3-[(3-cholamidopropyl)dimethylammonio]-1-propanesulfonate (Chaps), a different detergent, had a similar effect (data not shown). The addition of irrelevant proteins, such as BSA, increases the anisotropy (Fig. 3D), which might result from a combination of increasing viscosity and a potential weak interaction between FAM-peptide and BSA.

#### pH effect

The effects of pH have been recognized in a number of 14-3-3 target interactions [22–24]. Because the reported assays were not based on the binding itself or were based only within a limited pH range, the effect of pH on 14-3-3-mediated binding remains elusive. In the homogeneous solution assay, the anisotropy value for the binding of FAM-RGRSWpTY-COOH to 14-3-3 $\zeta$  varied from 45 at pH 9.0 to around 155 at pH 6.0–6.5 (Fig. 4A). Within this pH range, FAM-RGRSWpTY-COOH alone showed no significant change in anisotropy. In contrast, the fluores-

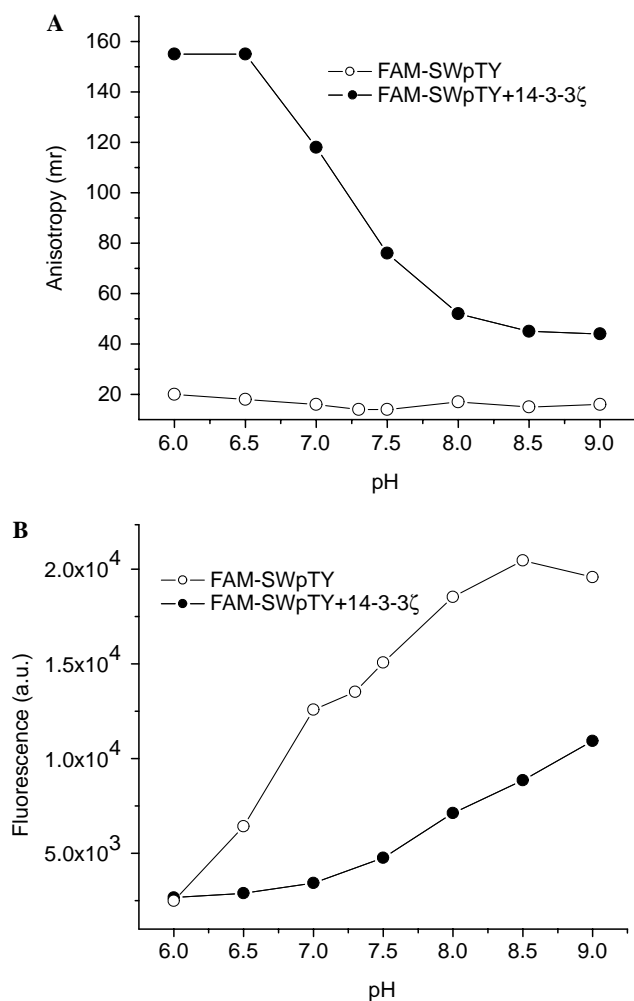


Fig. 4. pH effect on the fluorescence anisotropy and intensity. (A) Anisotropy signal (vertical axis) is plotted against different pH in the presence (●) or absence (○) of 14-3-3 $\zeta$  (as indicated). (B) Fluorescence intensity signal (vertical axis) is plotted against different pH in the presence (●) or absence (○) of 14-3-3 $\zeta$  (as indicated). The experiment was performed with 0.8  $\mu$ M FAM-RGRSWpTY-COOH and 0.68  $\mu$ M 14-3-3 $\zeta$  in a total volume of 100  $\mu$ l of the buffered pH.

cence intensity increases as pH increases from 6.0 to 9.0 (Fig. 4B). The difference in pH sensitivity for the free and bound FAM-RGRSWpTY-COOH likely causes the apparent reduction of fluorescence intensity upon 14-3-3 binding at pH 7.3 (Fig. 1A).

#### Sensitivity of the homogeneous assay

For detection in anisotropy, the limit of detection (LOD;  $S/N = 3$ ) for 14-3-3 $\zeta$  is 16 nM, with a linear range of 16–700 nM (Fig. 5A). The linear range could be improved by increasing the concentration of the labeled peptide. Conversely, LOD for FAM-RGRSWpTY-COOH is 0.68  $\mu$ M with a linear range of 0.68–2  $\mu$ M in the presence of 14-3-3 $\zeta$  (Fig. 5B).

If detected with the fluorescence intensity, LOD for FAM-SWpTY can reach as low as 0.14 nM in the absence of 14-3-3 $\zeta$  and 0.33 nM in the presence of 14-3-3 $\zeta$  (Fig. 5C).

The difference in LODs is mainly due to the interference from the light scattering, as shown in Fig. 5D. Only at a concentration higher than 2–5 nM will the interference be minimal.

#### Determination of the binding affinity

The binding assay has been applied to determine the dissociation constant of 14-3-3 with fluorescein-labeled FAM-RGRSWpTY-COOH or free unlabeled peptides [13]. To compare the  $K_D$  constants of different measurement methods, we synthesized and compared the affinity of a series of peptides, including the two binding sites of Raf1 (S259, S621) [8,9], the C-terminal binding site of arylalkylamine *N*-acetyltransferase (AANAT) [11], R18 [16], and SWTY peptides in either phosphorylated or unphosphorylated form [14] (Table 1). The ranking order of affinity is consistent with the reported values (Table 2). The absolute values, however, are generally lower than those obtained by solid-phase-based measurements (Fig. 6, Tables 1 and 2). In the case of the C-terminal peptide of plant plasma membrane  $H^+$ -ATPase, the dissociation constant ( $K_D$ ) is 2.5  $\mu$ M by isothermal titration microcalorimetry [12], comparable to the  $K_D$  of 6.0  $\mu$ M (wild-type) and 2.5  $\mu$ M (Q-5R) obtained in our competition fluorescence anisotropy assay (Table 1). This supports the notion that the solution-based measurement used here is more consistent with that obtained by microcalorimetry.

#### Monitoring 14-3-3 binding in crude cell lysate

To monitor the binding of peptide to native 14-3-3 proteins, homogeneous solution assays were applied for testing the FAM-RGRSWpTY-COOH interaction with crude cell lysate. Increased anisotropy signal of the FAM-RGRSWpTY-COOH was detected in the presence of crude cell lysate. The increase of anisotropy correlates with the concentration of protein in the lysate. In contrast, denatured cell lysate displayed a reduced signal of anisotropy (Fig. 7A). To affirm that signal differences in native and denatured protein preparation corresponds to the specific binding, R18 peptide was used to compete with FAM-RGRSWpTY-COOH for 14-3-3 binding. The difference in anisotropy in signals in the absence and presence of R18 should represent specific 14-3-3 binding signal. Indeed, the addition of R18 reduces the anisotropy to a level comparable to that of denatured lysate (Fig. 7A). The overall anisotropy signal was further enhanced when the cell lysates were spiked with recombinant 14-3-3 $\zeta$ . Consistently, the specific fraction of the signal was eliminated by R18 peptide and anisotropy was reduced to the same level as that of denatured cell lysate (Fig. 7A).

Using unlabeled RGRSWpTY-COOH peptides, we found comparable values of  $K_D$  for the recombinant 14-3-3 $\zeta$  and the native 14-3-3s in the cell lysate (data not shown). This provides evidence of similar affinity, hence allowing for estimation of the amount of 14-3-3 in cell

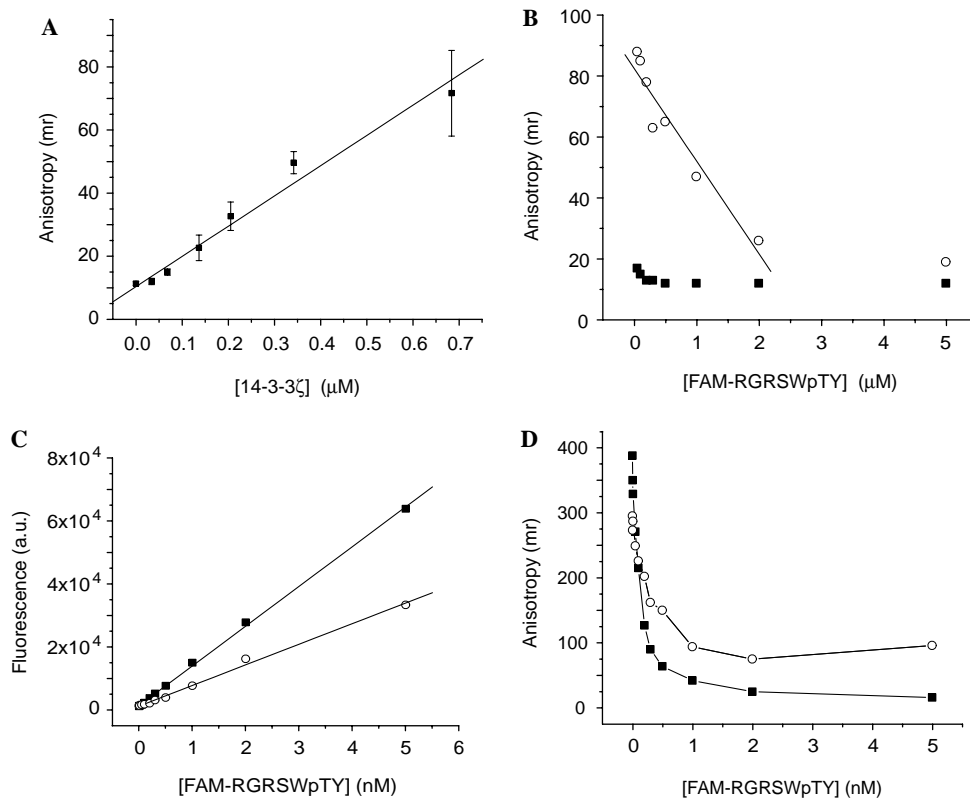


Fig. 5. Assay sensitivity. (A) Fluorescence anisotropy calibration of 14-3-3 $\zeta$ . The experiment was performed with 0.2  $\mu$ M FAM-RGRSWpTY-COOH in a total volume of 100  $\mu$ l. (B) Fluorescence anisotropy calibration of FAM-RGRSWpTY-COOH. The experiment was performed with 0.68  $\mu$ M 14-3-3 $\zeta$  in a total volume of 100  $\mu$ l. -○- with 14-3-3 $\zeta$ ; -■- without 14-3-3 $\zeta$ . (C) Fluorescence intensity calibration of FAM-RGRSWpTY-COOH. The experiment was performed with 0.68  $\mu$ M 14-3-3 $\zeta$  in a total volume of 100  $\mu$ l. -○- with 14-3-3 $\zeta$ ; -■- without 14-3-3 $\zeta$ . (D) Fluorescence anisotropy response at low nM concentrations of FAM-RGRSWpTY-COOH. The experiment was performed with 0.68  $\mu$ M of 14-3-3 $\zeta$  in a total volume of 100  $\mu$ l. Symbols of -○- and -■- indicate either with and without 14-3-3 $\zeta$ .

lysates that are available for interaction. To determine the total available 14-3-3 proteins in cell lysate, a calibration curve was generated by spiking the denatured cell lysate with 14-3-3 $\zeta$  (Fig. 7B and Materials and methods). The experiments have a LOD (S/N = 3) of 47 nM and linear range between 47 and 700 nM. The detection of the 14-3-3 in cell lysate resulted in a concentration of 0.13  $\mu$ M for the crude lysate. The immunoblot using specific antibody and known amounts of recombinant 14-3-3 protein yielded an estimated concentration of 0.17  $\mu$ M for 14-3-3 in the cell lysate (Figs. 7C and D).

#### High-throughput compatibility of the binding assay

The compatibility with the HTS was evaluated in a 384-well plate format. The assay can tolerate up to 10% dimethyl sulfoxide with the change of anisotropy less than 10%. In a 100  $\mu$ l reaction volume, the Z factor values as calculated from FAM-RGRSWpTY-COOH alone and FAM-RGRSWpTY-COOH saturated with 14-3-3 $\zeta$  are 0.62 in 20-data-point sets. The assay has a robust signal-to-noise ratio of  $\sim$ 7. The assay volume may be reduced to 20  $\mu$ l with a satisfactory Z factor of 0.51 (Figs. 8A and B). These parameters indicate that the anisotropy measurement is a robust HTS assay.

#### Discussion

Several methods have been developed for the binding assays of 14-3-3 due to its diverse importance in biological functions [7]. Some commonly used in vitro assays for 14-3-3 proteins are summarized in Table 2. Radioactive binding assays, which measure the binding of 14-3-3 with either  $^{32}$ P-labeled phosphorylated peptides or radiolabeled 14-3-3, have high sensitivities and are compatible with a good throughput format. Label-free methods, including SPR and calorimetric assay, have also been used in the 14-3-3 binding assays. In particular, calorimetry is probably most accurate despite the requirement of large amounts of reaction materials. The throughput remains to be a major challenge preventing these assays from having a broad application. Because 14-3-3 binding to enzymes often causes a change of catalytic activity, this feature has been used elegantly to test the interaction and estimate the affinity. It is especially successful for weak interactions and measuring subtle changes in the affinity (e.g., [11]) Because of the requirements for radioactivity, target specificity, or substantial amounts of pure proteins for these methods, a more general approach with improvements in the above-mentioned requirements is needed.

Table 2  
Binding assays and  $K_D$  comparison

Mode	Peptide sequences/proteins <sup>a</sup>	Methods <sup>b</sup>	14-3-3	$K_D$ (nM)	Ref.
Mode I RSx (pS/pT) xP <sup>c</sup>	RSRSTpSTP (pS-Raf259)	SPR	14-3-3 $\eta$ -GST	510	[9]
	RSApSEP (pS-Raf621)	SPR	14-3-3 $\eta$ -GST	1270	[9]
	RSRSTSTP (Raf259)	SPR	14-3-3 $\eta$ -GST	>50,000	[9]
	LSQRQTSTpSTPNVHM (pS-Raf259)	SPR	14-3-3 $\eta$ -GST	116	[9]
	LSQRQTSTpSTPNVHM (pS-Raf259)	SPR	14-3-3 $\eta$ -GST	128	[8]
	LSQRQTSTpSTPNVHM (pS-Raf259)	SPR	14-3-3 $\zeta$ -GST	122	[8]
	LSQRQRSTpSTPNVHMV (pS-Raf259)	FRET	14-3-3 $\zeta$	124	[18]
	AANAT (pT31)	RBA	GST-14-3-3 $\zeta$	31.8	[11]
	Nitrate reductase	Enzyme coupling	His-BMH <sup>a</sup>	2.5	[26]
	CGPTLKRTApSTPFM				
	Nitrate reductase PNR6	SPR	His-GF14 $\omega$ <sup>a</sup>	843	[23]
Mode II R $\Phi$ x(pS/pT)xP <sup>c</sup>	Biotin-MAGGGRLSHpSLP	SPR	14-3-3 $\eta$ -GST	55.7	[9]
	Biotin-MAGGGRLYHpSLP	SPR	14-3-3 $\eta$ -GST	37.4	[9]
	Biotin-MAGGGRLSHpSLG	SPR	14-3-3 $\eta$ -GST	190.4	[9]
	AcNH-RL $\Omega$ RpSLPA-CONH2 <sup>d</sup>	FI	14-3-3 $\zeta$ -GST	4600	[17]
Mode III pS/pT(X <sub>1-2</sub> )-COOH	Biotin-VKLKGLDIETPSHYpTV-COOH (BA-(933–948)-P, AHA2)	SPR	GF14 $\omega$	88	[27]
	QSYpTV-COOH (PMA2)	ITM	His-14-3-3c	2500 <sup>e</sup>	[12]
	QSYpTVP-COOH	ITM	His-14-3-3c	2700 <sup>e</sup>	[12]
	QSYpT-COOH	ITM	His-14-3-3c	15,000 <sup>e</sup>	[12]
	AANAT (pS205)	RBA	GST-14-3-3 $\zeta$	21.7	[11]
	2 Binding sites	MAGGGGRSApSEP-(AHA) <sub>6</sub> -RSApSEPAKK	SPR	14-3-3 $\eta$ -GST	~20
AANAT (pT31, pS205)		RBA	14-3-3 $\zeta$ -GST	7.2	[11]
Unphosphorylated peptides	KEESEK-COOH (Ammodytotoxin C)	SPR <sup>f</sup>	14-3-3	1000 <sup>g</sup>	[28]
	<sup>245</sup> FGADAE <sup>g</sup> , $\Delta$ N222, ExoS	SPR	His-14-3-3 $\zeta$	7.2	[29]
	H <sub>2</sub> N-PHCVPRDLSWLDLEANMCLP-COOH (R18)	RBA	14-3-3 $\zeta$ -GST	90	[15]

<sup>a</sup> AANAT, arylalkylamine *N*-acetyltransferase; AHA2, *Arabidopsis* plasma membrane H<sup>+</sup>-ATPase; PMA2, plasma membrane H<sup>+</sup>-ATPase; ExoS, ADP-ribosyltransferase exoenzyme S; BMH, yeast 14-3-3; GF14 $\omega$ , plant 14-3-3 (tobacco).

<sup>b</sup> SPR, surface plasmon resonance, with immobilized peptides; FRET, fluorescence resonance energy transfer; RBA, radioactive binding assay; FI, fluorescence intensity; ITM, isothermal titration microcalorimetry.

<sup>c</sup> Uppercase indicates a highly conserved position;  $\Phi$ , an aromatic or aliphatic amino acid; x, any amino acid.

<sup>d</sup>  $\Omega$ , fluorophore-labeled amino acid.

<sup>e</sup> pH 6.5 with Mg<sup>2+</sup> and Ca<sup>2+</sup>.

<sup>f</sup> Immobilized 14-3-3.

<sup>g</sup> pH 8.2 with Mg<sup>2+</sup> and Ca<sup>2+</sup>.

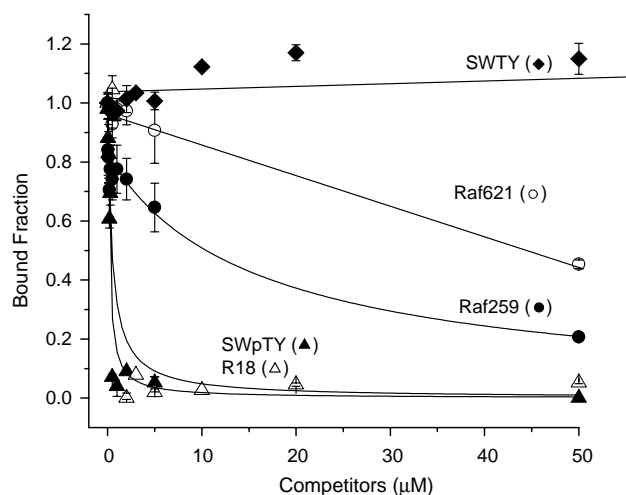


Fig. 6. Competition analyses using unlabeled peptides. Normalized signal of anisotropy (vertical axis) in the presence of indicated peptides is plotted against concentration of competitive peptides (horizontal axis). The detection was performed in triplicate. ● Raf259; ○ Raf621; ▲ SWpTY; △ R18; ◆ SWTY. The sequences of referenced peptides are shown in Table 1.

Considering the reported solution-based assays, microcalorimetry is a highly reliable approach to determine absolute affinity, but it requires considerable amounts of materials. On the other hand, environment-sensitive fluorescent amino acids have been synthesized and incorporated into 14-3-3 binding peptides to monitor 14-3-3 binding [25]. A Förster-resonance-energy-transfer-(FRET)-based binding assay has also been explored using a binding peptide and 14-3-3 protein that are both labeled with fluorophores [26]. However, the uniqueness of fluorophore and mutated 14-3-3 hampers the general use of FRET for determining binding affinity. The fluorescence anisotropy method reported here represents a major step of improvement for in vitro analyses of 14-3-3 interactions. First, the sensitivity and experimental procedures are significantly improved by measuring anisotropy. The SWTY peptide recognizes the same binding groove as that of canonical peptide substrates [13,14]. Hence, the competition assay described here (Fig. 6 and Table 1) should be generally applicable to other interactions involving canonical peptide

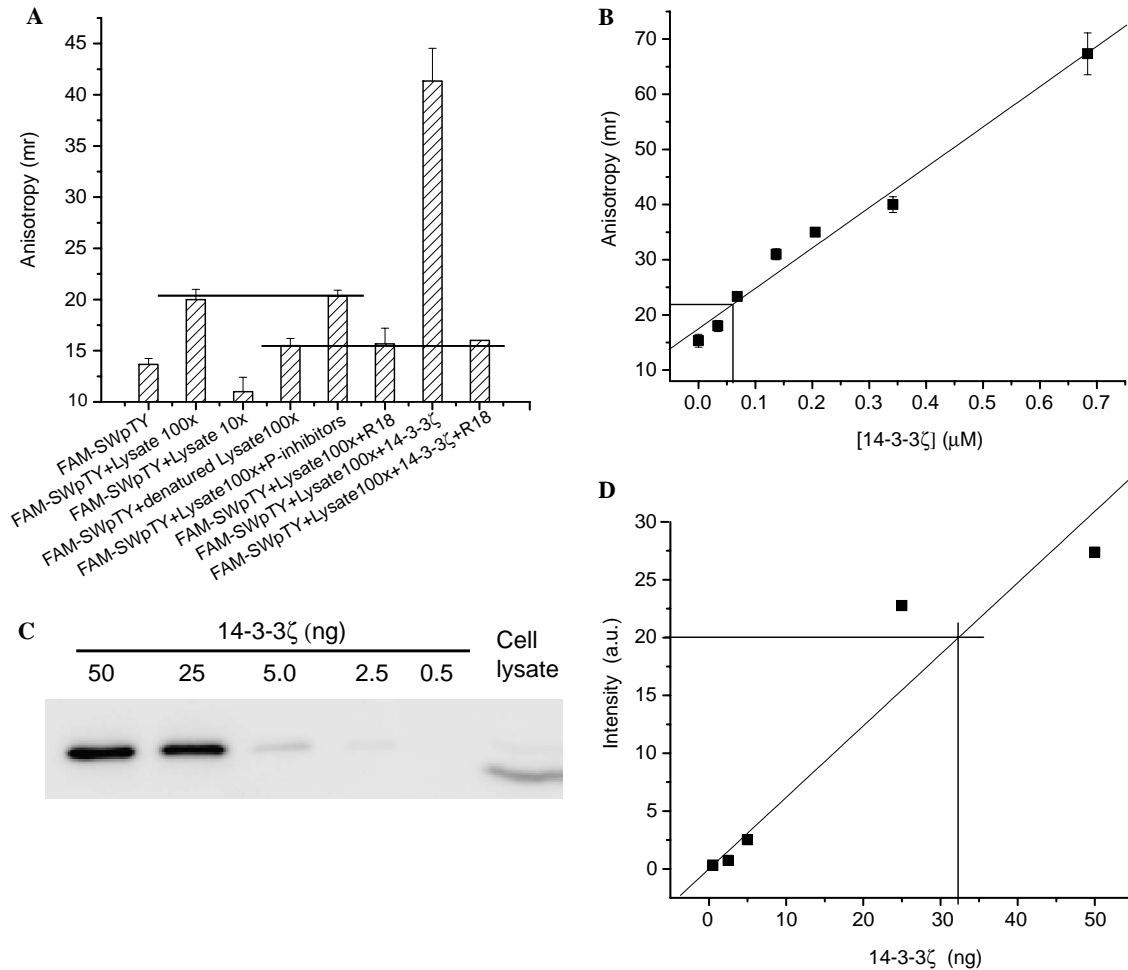


Fig. 7. Specific detection of 14-3-3 in cell lysate. (A) Specificity of 14-3-3 responses from FAM-RGRSWpTY-COOH interaction with cell lysate. Lysate 100 $\times$  as 0.14 mg/ml of protein, 10 $\times$  as 0.014 mg/ml, P-inhibitors as phosphatase inhibitors of 50 mM NaF and 1 mM sodium orthovanadate. The experiments were performed in triplicate. (B) Fluorescence anisotropy calibration of spiked 14-3-3 $\zeta$  in denatured cell lysate and 14-3-3 detection in cell lysate. (C) Immunoblot of indicated amounts of recombinant 14-3-3 $\zeta$  and native 14-3-3 in cell lysate. (D) Quantification of native 14-3-3 in cell lysate. The band intensity of immunoblotted recombinant 14-3-3 $\zeta$  was quantitated and plotted for the calibration curve. Native 14-3-3 was quantitated through the calibration curve by the band intensity of cell lysate.

binding to 14-3-3. Second, the absolute values determined by this approach are homogeneous solution based, which gives rise to more accurate dissociation constants. In addition, the assay is compatible to either pure or crude protein preparations. This may be particularly useful for monitoring 14-3-3 binding activities under different biochemical conditions. Third, the throughput of this assay is considerably higher than that of any of the existing assays. The measurement is performed without filtering, electrophoresis, or precipitation steps. Since rigorous incubation time and temperature control are not necessary for the assay and reagent mixture is a simple stepwise liquid addition, it is conveniently adaptable to robotic manipulation. Because the signal-to-noise ratio remains desirable in as low as 20  $\mu$ l (Fig. 8) reaction volume, the assay may be further improved and applicable to 1536-well format.

The affinity and stability of FAM-RGRSWpTY-COOH peptide could affect the general utility of this probe. The dissociation constants ( $K_D$ ) are  $0.49 \pm 0.14 \mu$ M determined

by direct binding of the labeled peptide and  $0.17 \pm 0.04 \mu$ M by competition experiments using unlabeled peptide [13]. The dynamic range may be expanded by using FAM-labeled RGRSWpTG or RGRSWpTP peptides which have  $K_D$  values of  $1.5 \pm 0.01$  and  $45 \pm 11 \mu$ M (Table 1) [13]. The stability of the labeled peptide could be affected by ambient irradiation and potential phosphatase in the crude protein preparation. Our results suggest that the dephosphorylation was not a major concern under typical experimental conditions as shown in Fig. 8A. This perhaps should not be a surprise since the SWTY peptide was obtained by a general screen from yeast and tested in mammalian cells. Should it be sensitive to phosphatase, it may not be effective in recruiting 14-3-3. Future improvements may be sought by testing RGRSWpTY-COOH peptides conjugated with different fluorophores.

In conclusion, a homogeneous fluorescence-anisotropy-based 14-3-3 binding assay has been developed. The method permits a mix-and-read format to determine the

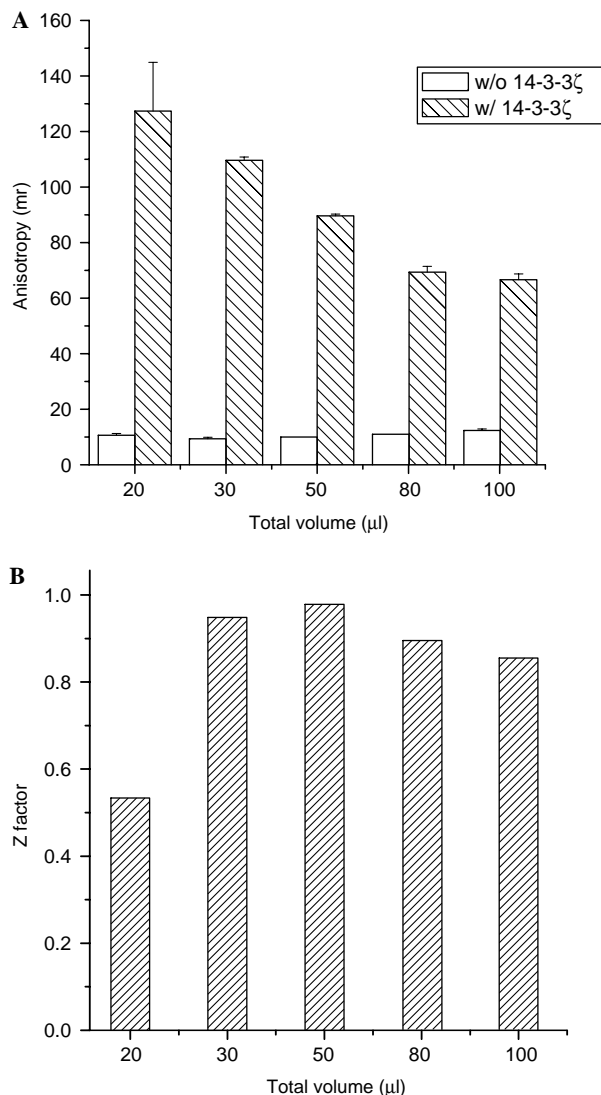


Fig. 8. Volume minimization and Z factor of the anisotropy detection. (A) Volume minimization with the identical concentration of FAM-RGRSWpTY-COOH (0.4  $\mu$ M) and 14-3-3 $\zeta$  (0.68  $\mu$ M) in total volumes of 100, 80, 50, 30, and 20  $\mu$ l. (B) Corresponding Z factors from different total volumes from experiments in (A).

dissociation constants of various peptides (or proteins) using a fluorescein-labeled peptide probe (FAM-RGRSWpTY-COOH). Assay conditions suitable for high-throughput screening have been evaluated. The robustness of the assay permits detection of 14-3-3 proteins in crude cell lysate. These advantageous features broaden its application to 14-3-3-involved interactions for both affinity measurement and high-throughput screening.

#### Acknowledgments

We thank members of the Li lab for valuable comments and discussions on the manuscript. The work is supported by grants from the National Institutes of Health (GM70959 and NS33324 to M.L.; GM53165 and GM60033 to H.F.), a technology development award from

Corning (to M.L.), a predoctoral fellowship award from the American Heart Association (B.C.), and Johns Hopkins ChemCORE facility.

#### References

- [1] M.B. Yaffe, How do 14-3-3 proteins work?—Gatekeeper phosphorylation and the molecular anvil hypothesis, *FEBS Lett.* 513 (2002) 53–57.
- [2] M.K. Dougherty, D.K. Morrison, Unlocking the code of 14-3-3, *J. Cell Sci.* 117 (2004) 1875–1884.
- [3] H. Fu, R.R. Subramanian, S.C. Masters, 14-3-3 proteins: structure, function, and regulation, *Annu. Rev. Pharmacol. Toxicol.* 40 (2000) 617–647.
- [4] A. Aitken, H. Baxter, T. Dubois, S. Clokie, S. Mackie, K. Mitchell, A. Peden, E. Zemlickova, Specificity of 14-3-3 isoform dimer interactions and phosphorylation, *Biochem. Soc. Trans.* 30 (2002) 351–360.
- [5] A.J. Muslin, J.M.C. Lau, Academic Press, 2004, pp. 211–228.
- [6] A.J. Aksamit Jr., C.M. Preissner, H.A. Homburger, Quantitation of 14-3-3 and neuron-specific enolase proteins in CSF in Creutzfeldt–Jakob disease, *Neurology* 57 (2001) 728–730.
- [7] E. Wilker, M.B. Yaffe, 14-3-3 Proteins—a focus on cancer and human disease, *J. Mol. Cell. Cardiol.* 37 (2004) 633–642.
- [8] A.J. Muslin, J.W. Tanner, P.M. Allen, A.S. Shaw, Interaction of 14-3-3 with signaling proteins is mediated by the recognition of phosphoserine, *Cell* 84 (1996) 889–897.
- [9] M.B. Yaffe, K. Rittinger, S. Volinia, P.R. Caron, A. Aitken, H. Leffers, S.J. Gamblin, S.J. Smerdon, L.C. Cantley, The structural basis for 14-3-3:phosphopeptide binding specificity, *Cell* 91 (1997) 961–971.
- [10] A.T. Fuglsang, J. Borch, K. Bych, T.P. Jahn, P. Roepstorff, M.G. Palmgren, The binding site for regulatory 14-3-3 protein in plant plasma membrane H<sup>+</sup>-ATPase: involvement of a region promoting phosphorylation-independent interaction in addition to the phosphorylation-dependent C-terminal end, *J. Biol. Chem.* 278 (2003) 42266–42272.
- [11] S. Ganguly, J.L. Weller, A. Ho, P. Chemineau, B. Malpoux, D.C. Klein, Melatonin synthesis: 14-3-3-dependent activation and inhibition of arylalkylamine N-acetyltransferase mediated by phosphoserine-205, *Proc. Natl. Acad. Sci. USA* 102 (2005) 1222–1227.
- [12] M. Wurtele, C. Jelich-Ottmann, A. Wittinghofer, C. Oecking, Structural view of a fungal toxin acting on a 14-3-3 regulatory complex, *EMBO J.* 22 (2003) 987–994.
- [13] B. Coblitz, S. Shikano, M. Wu, S.B. Gabelli, L.M. Cockrell, M. Spieker, Y. Hanyu, H. Fu, L.M. Amzel, M. Li, C-terminal recognition by 14-3-3 proteins for surface expression of membrane receptors, *J. Biol. Chem.* 280 (2005) 36263–36272.
- [14] S. Shikano, B. Coblitz, H. Sun, M. Li, Genetic isolation of transport signals directing cell surface expression, *Nat. Cell Biol.* 7 (2005) 985–992.
- [15] B. Hallberg, Exoenzyme S binds its cofactor 14-3-3 through a non-phosphorylated motif, *Biochem. Soc. Trans.* 30 (2002) 401–405.
- [16] B. Wang, H. Yang, L. YC, T. Jelinek, L. Zhang, E. Ruoslahti, H. Fu, Isolation of high-affinity peptide antagonists of 14-3-3 proteins by phage display, *Biochemistry* 38 (1999) 12499–12504.
- [17] B. Harris, B. Hillier, W. Lim, Energetic determinants of internal motif recognition by PDZ domains, *Biochemistry* 40 (2001) 5921–5930.
- [18] N. Macdonald, J.P. Welburn, M.E. Noble, A. Nguyen, M.B. Yaffe, D. Clynes, J.G. Moggs, G. Orphanides, S. Thomson, J.W. Edmunds, A.L. Clayton, J.A. Endicott, L.C. Mahadevan, Molecular basis for the recognition of phosphorylated and phosphoacetylated histone h3 by 14-3-3, *Mol. Cell* 20 (2005) 199–211.
- [19] M.A. Freulet-Marriere, G. Potocki-Veronese, J.R. Deverre, L. Sabatier, Rapid method for mean telomere length measurement directly from cell lysates, *Biochem. Biophys. Res. Commun.* 314 (2004) 950–956.
- [20] M.M. Bradford, A rapid and sensitive method for the quantitation of microgram quantities of protein utilizing the principle of protein dye binding, *Anal. Biochem.* 72 (1976) 248–254.

- [21] S.A. Kane, C.A. Fleener, Y.S. Zhang, L.J. Davis, A.L. Musselman, P.S. Huang, Development of a binding assay for p53/HDM2 by using homogeneous time-resolved fluorescence, *Anal. Biochem.* 278 (2000) 29–38.
- [22] G.S. Athwal, S.C. Huber, Divalent cations and polyamines bind to loop 8 of 14-3-3 proteins, modulating their interaction with phosphorylated nitrate reductase, *Plant J.* 29 (2002) 119–129.
- [23] D.M. Bustos, A.A. Iglesias, A model for the interaction between plant GAPN and 14-3-3[zeta] using protein–protein docking calculations, electrostatic potentials and kinetics, *J. Mol. Graphics Model.* 23 (2005) 490–502.
- [24] A. Kandlbinder, H. Weiner, W.M. Kaiser, Nitrate reductases from leaves of *Ricinus* (*Ricinus communis* L.) and spinach (*Spinacia oleracea* L.) have different regulatory properties, *J. Exp. Bot.* 51 (2000) 1099–1105.
- [25] M. Eugenio Vazquez, D.M. Rothman, B. Imperiali, A new environment-sensitive fluorescent amino acid for Fmoc-based solid phase peptide synthesis, *Org. Biomol. Chem.* 2 (2004) 1965–1966.
- [26] J. Silhan, V. Obsilova, J. Vecer, P. Herman, M. Sulc, J. Teisinger, T. Obsil, 14-3-3 Protein C-terminal stretch occupies ligand binding groove and is displaced by phosphopeptide binding, *J. Biol. Chem.* 279 (2004) 49113–49119.
- [27] A.T. Fuglsang, S. Visconti, K. Drumm, T. Jahn, A. Stensballe, B. Mattei, O.N. Jensen, P. Aducci, M.G. Palmgren, Binding of 14-3-3 Protein to the Plasma Membrane H<sup>+</sup>-ATPase AHA2 Involves the Three C-terminal Residues Tyr946-Thr-Val and Requires Phosphorylation of Thr947, *J. Biol. Chem.* 274 (1999) 36774–36780.
- [28] J. Sribar, N.E. Sherman, P. Prijatelj, G. Faure, F. Gubensek, J.W. Fox, A. Aitken, J. Pungercar, I. Krizaj, The neurotoxic phospholipase A2 associates, through a non-phosphorylated binding motif, with 14-3-3 protein  $\gamma$  and  $\epsilon$  isoforms, *Biochem. Biophys. Res. Commun.* 302 (2003) 691–696.
- [29] L. Zhang, H. Wang, S.C. Masters, B. Wang, J.T. Barbieri, H. Fu, Residues of 14-3-3 zeta required for activation of exoenzyme S of *Pseudomonas aeruginosa*, *Biochemistry* 38 (1999) 12159–12164.